Meas. Sci. Technol. 4 (1993) 311–320. Printed in the UK

A new laser voltmeter

M Abd-Elsalam†, M Abdel-Salam‡, D Wiitanen§ and W Perger§

† Faculty of Engineering, 108 Shoubra St, Cairo, Egypt
‡ EE Department, KFUPM, Dhahran 31261, Saudi Arabia
§ EE Department, Michigan Tech, Houghton, MI 49931, USA

Received 1 July 1992, in final form 8 October 1992, accepted for publication 22 October 1992

Abstract. This paper presents a new laser voltmeter employing a novel Kerr cell for remote measurement of high voltages. Unlike conventional Kerr cells, the proposed cell has no electrodes and is merely a vessel filled with an optically-active liquid. The cell is placed in the strong-field zone of a gap stressed by the voltage under measurement. Optical measurement of the liquid Kerr retardation angle reflects the electric-field value inside the cell which expresses the measured voltage. A sensitive optical system has been used for measuring Kerr retardation angles down to 0.01 degrees.

A 'Figure of Merit' has been proposed to express the sensitivity of the optical liquid. The figure of merit depends on both the Kerr and dielectric constants of the liquid. As a new liquid having a relatively low dielectric constant, chlorotoluene is found to be promising. Its figure of merit is 2.48 times that of nitrobenzene which has the highest Kerr constant among the common liquids. Also, it is found that chlorotoluene is more stable and easier to purify than nitrobenzene.

The laser voltmeter has been tested experimentally in uniform- and non-uniform-field gaps. Optical measurement of the AC voltage applied to the gap electrodes agreed well with that obtained by a calibrated potential divider.

1. Introduction

The basic principle of remote measurement of high voltages using the Kerr effect were inspired by the principle of conventional Kerr cells [1]. The conventional Kerr cell has two parallel plates immersed in an optically active liquid as shown in figure 1. The high voltage V, which is to be measured, is applied directly to the plates (electrodes) through suitable insulation. The electric field $E(L)$ between the electrodes interacts with the liquid, so that the polarized light passing through the liquid is retarded by the Kerr retardation angle γ. The relation between the applied field and the Kerr retardation angle is expressed [2] as

$$\gamma = 2\pi B_k \int_0^L E^2(L)\,dl \qquad (1)$$

where γ is the Kerr retardation angle in radians, B_k is the Kerr constant of the liquid (in m V^{-2}), $E(L)$ is the electric field inside the cell normal to the plane of light propagation (in V m^{-1}), and L is the cell length which is subjected to the electric field $E(L)$ and through which the light propagates (in m). If the electric field $E(L)$ is uniform and has a constant value E along the optical path length L, equation (1) reduces to

$$\gamma = 2\pi B_k L E^2 \qquad (2)$$

The widely used optical system [3] for measuring Kerr retardation angles γ is shown in figure 1. In this system, two crossed polarizers are used. The first polarizer, placed between the light source and the cell, is oriented at 45° to the direction of the applied field. However, the analyzing polarizer, placed between the cell and the photo-detector, is oriented perpendicular to the first polarizer, i.e. at −45° to the direction of the field. If the optical losses are neglected and P_0 is taken as the intensity of the light source, the output intensity P detected by the photo-detector is found by Mueller

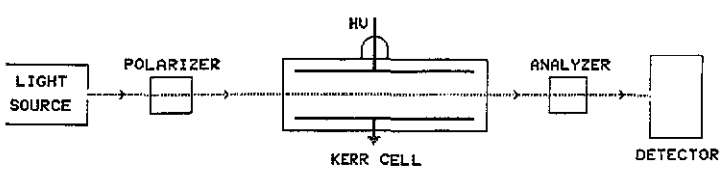

Figure 1. A conventional Kerr cell and the traditional optical system for measuring Kerr retardation angles.

0957-0233/93/030311+10 $07.50

matrix formalism [4, 5] as:

$$P = \frac{P_0}{4} \sin^2 \frac{\gamma}{2}. \tag{3}$$

Although employing Kerr cells for high-voltage measurement provides a broad frequency response, they have drawbacks. These drawbacks are basically attributed to applying the high-voltage directly to the immersed electrodes and may be summarized as follows:

(1) At high electric fields, conduction currents are produced and result in excessive heating of the liquid which leads to thermal instability [6].
(2) Using immersed electrodes leads to formation of space charges near the electrodes which distort the field. This disortion is influenced by the level, frequency and duration of the applied voltage and also is affected by the electrode material [7].
(3) Because of the capacitance of the two parallel electrodes and their associated leads, the conventional Kerr cell may not be adequate for measurements of very fast pulses [4].
(4) Because the voltage which is to be measured is connected directly to the immersed electrodes, expensive insulation is required.

To avoid these drawbacks, a novel technique is proposed which employs a new Kerr cell. Such a cell has no electrodes and is merely a vessel filled with the optically active liquid.

Other optical high voltage/electric field sensors have been reported [8, 9] in the literature. An integrated optics Mach–Zehnder interferometer in conjunction with a capacitive divider has been proposed [8] for measuring high voltages such as those encountered in SF_6 gas-insulated bus ducts. A CW electro-optic probing technique has been suggested [9] for studying electric-field distribution in devices and in integrated circuits.

2. The proposed technique

The proposed technique is simply based on placing the new electrodeless Kerr cell in the strong-field zone of a gap stressed by the voltage to be measured (figure 2). The new cell serves to sense the electric field in the gap with no need for electrodes. The laser source and all of the detection electronic circuits are at ground potential. Therefore, the measuring circuit is electrically isolated from the high-voltage circuit, since the light beam provides the only connecting link.

To measure the high voltage applied to a conductor-to-plane gap, the cell is located underneath the conductor so that the value of the field inside the cell is strong enough to produce a suitable retardation angle γ but not so strong as to cause conduction currents in the bulk of the liquid. Therefore, this technique can be used to measure a wide range of conductor voltages by choosing a suitable location for the cell underneath the conductor.

2.1. Operating principles

Because the proposed technique measures only the electric field E inside the cell and because it is desired to measure the conductor voltage V and not the field, the relation between V and E should be known. This relation may be called the 'field-to-voltage ratio' and denoted by K_E, i.e.

$$K_E = E/V \quad (\mathrm{m}^{-1}). \tag{4}$$

Substituting E from equation (4) into equation (2) gives

$$\gamma = 2\pi B_k L K_E^2 V^2. \tag{5}$$

For AC voltage application, the instantaneous value v is expressed as

$$v = \sqrt{2}\, V_{RMS} \sin(\omega t)$$

where V_{RMS} is the root mean square value in volts, and ω is the angular frequency in radian $\sec^{-1}$.

Substituting into equation (5), the instantaneous value of the Kerr retardation angle $\gamma(t)$ yields

$$\gamma(t) = 4\pi B_k L K_E^2 V_{RMS}^2 \sin^2 \omega t \tag{6}$$

Equation (6) shows that the value of the retardation angle is time-varying with a peak value of

$$\gamma_{peak} = 4\pi B_k L K_E^2 V_{RMS}^2. \tag{7}$$

The above quadratic relation between the Kerr retardation angle and the applied voltage is the principal relation for voltage measurement using the proposed technique. By employing a suitable optical system for measuring the Kerr retardation angle, the voltage can be measured as:

$$V_{RMS} = \frac{\sqrt{\gamma_{peak}}}{\sqrt{4\pi B_k L (K_E)^2}}. \tag{8}$$

Therefore, the Kerr constant B_k and the field-to-voltage ratio K_E are prerequisites for the optical measurement of voltages.

2.2. Figure of merit as a guide for selecting the cell liquid

In the case of a conventional Kerr cell, the field between the two parallel-plate electrodes is uniform and given by $E = V/d$, where d is the distance between the plates. Therefore, the corresponding field-to-voltage ratio K_E of equation (4) yields

$$K_E = 1/d \quad (\mathrm{m}^{-1}) \tag{9}$$

Substituting K_E in equation (7)

$$\gamma_{peak} = 4\pi B_k L (1/d)^2 V_{RMS}^2. \tag{10}$$

It is clear from equation (10) that the retardation angle γ measured by a conventional cell is directly proportional to the Kerr constant of the liquid, i.e. the sensitivity of the liquid depends only on the Kerr constant of the liquid. Therefore, nitrobenzene is the most commonly

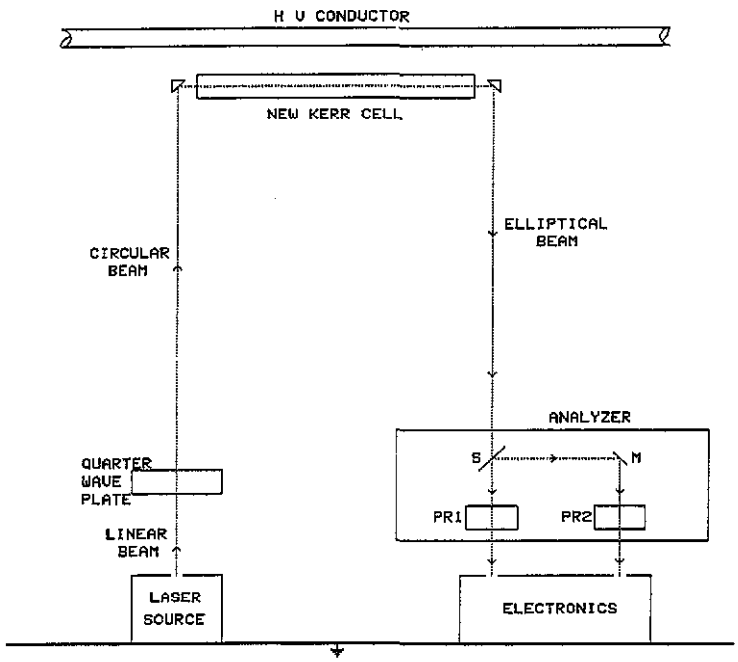

Figure 2. A schematic diagram for the proposed technique and the proposed optical system for measuring Kerr retardation angles: S, splitter; PR1, PR2, polarizers.

used liquid in conventional Kerr cells because of its high Kerr constant.

However, the sensitivity of the liquid used in the proposed electrodeless cell is more complicated. As shown in figure 2, the electrodeless Kerr cell is placed between the high-voltage conductor and ground. This is a two-dielectric system with the air around the cell and the liquid in it. The field inside the cell is affected by the location of the cell and the ratio of the permittivity of liquid to that of air, i.e. by the dielectric constant ε_r of the liquid. The field has been calculated in this system and it is found that the value of the field inside the cell is approximately inversely proportional to the value of the dielectric constant of the liquid (figures 3 and 4). Therefore the field-to-voltage ratio K_E is proportional to $1/\varepsilon_r$ for a cell having a particular location. Substituting K_E in equation (7)

$$\gamma_{peak} \propto 4\pi L V_{RMS}^2 B_k (1/\varepsilon_r^2). \tag{11}$$

Equation (11) dictates that, for a cell having a specific length and location, the retardation angle γ is directly proportional to the Kerr constant and inversely proportional to the squared value of the dielectric constant of the liquid, i.e.

$$\gamma \propto B_k/\varepsilon_r^2. \tag{12}$$

Therefore the ratio B_k/ε_r^2 is a measure of the liquid sensitivity and may be considered a 'figure of merit' for liquids used in the proposed cell.

2.3. Retardation angle measurements

The field inside the electrodeless cell should be weak enough to avoid conduction currents in the liquid. This can be accomplished by placing the cell relatively far away beneath the high-voltage conductor. However, according to equation (2), small retardation angles result from applying weak fields inside the cell. Since the traditional optical system used with conventional Kerr cells of figure 1 is not sensitive enough to measure small retardation angles, a new optical system has been proposed.

The new optical system has been inspired by the system adopted for measuring Pockel's retardation angles [10]. Figure 2 shows a schematic diagram of the

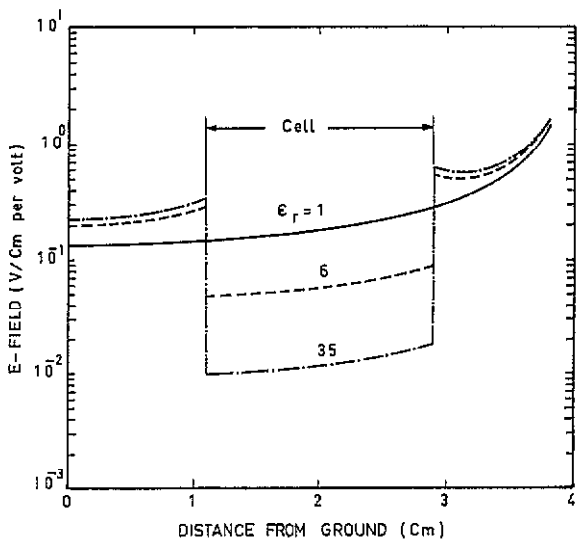

Figure 3. Electric fields ((V cm^{-1}) for 1 V applied to the wire) inside and outside an electrodeless Kerr cell placed between wire and ground and filled with liquids having a dielectric constant of 1, 6 and 35.

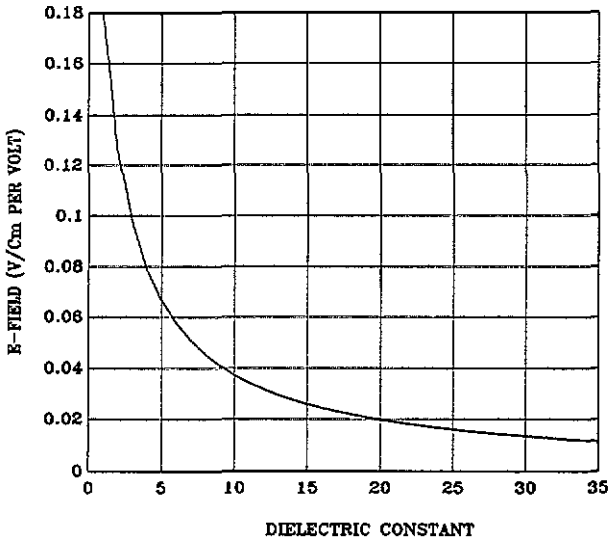

Figure 4. Electric field in the centre of an electrodeless Kerr cell, placed between wire and ground, versus the dielectric constant of the liquid filling the cell.

proposed optical system. A laser beam, which is a linearly polarized light, passes through a quarter-wave plate, with its slow axis at 45° to the plane of polarization of the laser-source beam, so that the linear beam changes into a circular one. The circular beam then passes through the Kerr cell placed in the electric field site. The electric field E interacts with the optical liquid in the cell, so that a Kerr retardation angle γ changes the circular beam into an elliptical one. The beam then passes through an analyser to determine the angle γ. The analyser splits the beam into two linearly orthogonal beams having polarization planes at $-45°$ and $+45°$ to the direction of the applied electric field, so that they have equal intensities P_1 and P_2, in the absence of the field, respectively. If the optical losses are neglected and P_0 is taken as the intensity of the laser source, the output intensities P_1 and P_2 leaving the analyser are found by Stokes parameters and Mueller matrix formalism [4, 5] as follows:

$$\left.\begin{aligned} P_1 &= \frac{P_0}{4}(1+\sin\gamma) \\ P_2 &= \frac{P_0}{4}(1-\sin\gamma). \end{aligned}\right\} \tag{13}$$

Taking the sum and difference, equation (13) leads to

$$\sin\gamma = \frac{P_1 - P_2}{P_1 + P_2}. \tag{14}$$

The advantages of the new optical system over the traditional system are as follows:

(1) In the traditional system, because of the optical loss, the maximum intensity $P_0/4$ of equation (3) must be calibrated because the instantaneous intensity P is related to the maximum intensity. However, in the new system, the retardation angle is related to the sum and the difference of the two split beams simultaneously, as given by equation (14). Therefore, the reading does not depend on the stability of the light source.

(2) In the new system, splitting the beam into two equal beams and obtaining the difference of their intensities minimises the noise of the resultant signal which has a value depending upon the common mode rejection ratio of the operational amplifiers employed. Since the minimum Kerr retardation angle that can be measured is limited by the noise, the new optical system is superior to the traditional system.

(3) From equation (3) of the traditional system, if the light source intensity P_0 is taken as unity, the modulation signal obtained by applying the field will be $0.25\sin^2(\gamma/2)$. However, the modulation signal for each beam of the new system is, from equation (14), $\pm 0.25\sin\gamma$ and for the difference of the two beams is $0.5\sin\gamma$. Figure 5 shows respectively the two modulation signals $0.25\sin^2(\gamma/2)$ and $0.5\sin\gamma$ of the traditional and new systems versus the retardation angle γ. It is quite clear that the sensitivity of the new system is much better than that of the traditional one.

Therefore, the new optical system is employed in all the experimental measurements either with conventional or new Kerr cells.

3. Implementation of the proposed measuring technique

3.1. Optical components

Figure 2 shows the optical components of the new optical system for measuring the Kerr retardation angle.

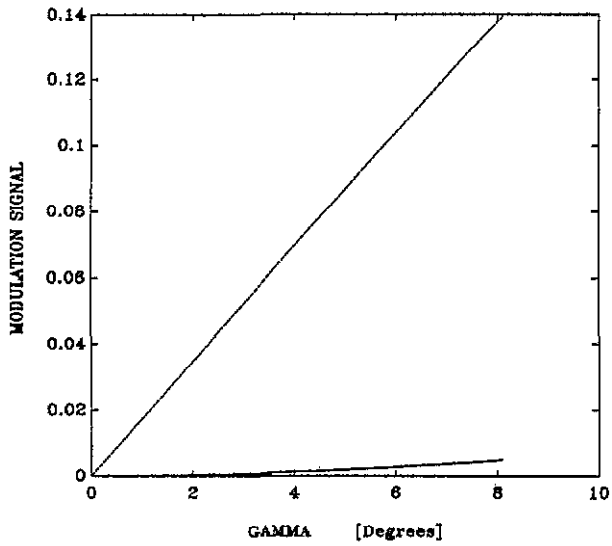

Figure 5. Comparison between the sensitivity of the new and the traditional optical systems for measuring Kerr retardation angles. The modulation signals (in arbitrary units) of (*a*) the traditional system ($0.25\sin^2(\gamma/20)$) (solid curve), and (*b*) the new system ($0.5\sin\gamma$) (broken curve).

A 15 mW Helium–Neon gas laser of 633 nm wavelength is employed for all measurements. A quarter-wave plate is placed after the laser source so that its slow axis makes 45° to the plane of polarization of the laser beam. For the analyser, a variable cylindrical splitter is used so that the split beams can be adjusted to have equal intensities in the absence of the field. The analyser also has two polarizers (Nicol prisms) aligned at $-45°$ and $+45°$ to the direction of the applied field directed along the x axis.

3.2. Detection electronics

According to equation (14), it is necessary to obtain the difference and the sum of the intensities of the two split beams. Therefore, two photodiodes and two operational amplifiers are employed (figure 6).

For measuring the intensity of the two split beams, ultrasensitive silicon photodiodes (UDT-620D, United Detector™) with built-in monolithic JFET operational amplifiers have been employed in order to allow low-level measurements and to ensure low-noise output. Since the output signal of the photodiode, by itself, is a current signal, the built-in operational amplifier is to change the signal from current to voltage signal.

To obtain the sum and difference of the two voltage signals of the photodiodes, precision amplifiers (AD624, Analog Devices™) have been used (figure 6), with a high common mode rejection ratio of 150 dB at a gain of 500 and above 80 dB at unity gain. The amplifier (AD624) does not need any external components for pretrimmed gains of 1, 100, 200, 500 and 1000. It has pin-programmable gain with low noise (0.2 μV p–p for 0.1 to 10 Hz). The two photodiodes and the operational amplifiers have been shielded by a metallic box in order to avoid picking up noise from the field applied to the Kerr cell. Also, two 12-volt automobile batteries are used as a power supply for the electronic circuits in order to avoid the 60 Hz noise.

Therefore, the detection electronics was designed to greatly reduce noise caused by amplitude fluctuations in the light source and other sources of noise. It does not necessarily reduce noise contributions from non-common mode sources such as the photodiodes and the electronics. This is why the precision of the photodiodes and the components of the detection electronics used in this work was the highest available commercially.

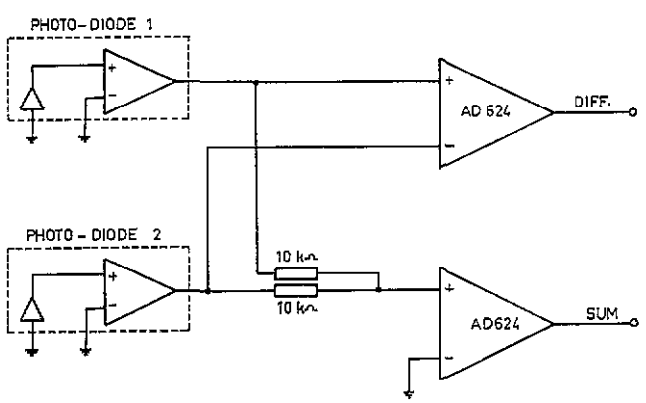

Figure 6. Details of the detection electronics circuit.

3.3. Test cells

Two cells A and B without electrodes have been built for the proposed measuring technique. Each cell is a glass tube 70 cm long. However they have two different radii R_d of 0.9 and 0.635 cm respectively (see figure 7).

A conventional Kerr cell C has been built to measure the Kerr constant of some optically active liquids. The cell is a glass tube 12 cm long and 2.54 cm in diameter. The cell is provided with two stainless steel parallel-plate electrodes each 10 cm long and 1 cm wide to apply the electric field. The two electrodes are held apart by a distance d of 1 cm by using two teflon spacers each 2 mm thick, one at each end of the electrodes.

4. Test arrangements and set-up

The voltage applied to the following two gaps (see figure 7):

(1) a uniform-field parallel-plate gap
(2) a non-uniform-field wire-to-plate gap

was measured optically using cells A and B and also by a calibrated potential divider.

For the two-parallel-plates gap, two identical stainless steel plates 50 cm long and 12.5 cm high are used. For the wire-to-plate gap, an aluminium conductor having a radius R_c of 0.3175 cm is used as a wire. The

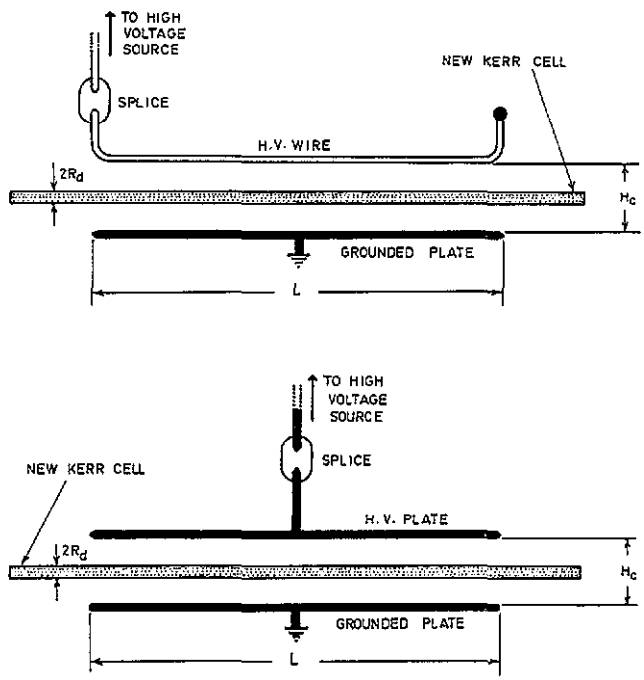

Figure 7. Experimental set-up showing the position of the cell relative to the electrodes of uniform- and non-uniform field gaps.

ends of the wire have been bent so that the effective length L of the wire is 50 cm. One of the wire ends is provided with a brass splice for connection to the high voltage source, while the other end is terminated by a small sphere in order to avoid local corona and sparks (figure 7). One of the plates of the two-parallel-plate arrangement is used for the wire-to-plate gap.

The cell and the electrodes stand on plexiglass supports held on a plexiglass base. The base has predetermined grooves so that the cell is always in the middle of the distance H_c between the electrodes, which can be accurately varied in the range 2–8 cm.

5. Results and discussion

5.1. Field-to-voltage ratio (K_E) determination

Each of the two gaps studied represents a two-dielectric system including the air surrounding the electrodes and the optical liquid inside the cell. Several numerical methods of determining the field in a system of two different dielectrics are available [11], including the finite element method, finite difference method, Monte Carlo method, moment method, method of images, and charge simulation method. The charge simulation method [12] is adopted here due to its inherent flexibility in matching the gaps studied. In order to simplify the calculation of the ratio K_E, the set-up, including the gap electrodes and the cell, has been considered infinitely long so that the field calculation procedure became a two-dimensional problem. The calculation of the field inside an electrodeless cell has been published before by the authors [13]. Table 1 gives the values of K_E of both gaps for different spacings between the electrodes H_c, using two cell radii R_d.

5.2. Figure of merit determination

Since nitrobenzene has the highest Kerr constant among common liquids ($B_k \cong 2.5 \times 10^{-12}$ m v^{-2} [5]), the 'figure of merit' for some known liquids has been determined in table 2 with respect to that of nitrobenzene. Although the Kerr constant of nitrotoluene is only 55% of that of nitrobenzene, its figure of merit is higher than that of nitrobenzene.

Trying new liquids having relatively low dielectric constant, chlorotoluene was found to be promising. Since the Kerr constant of chlorotoluene is not reported in the literature, its Kerr constant has been measured using the conventional cell C. Different values of V_{RMS} were applied to the cell electrodes and the corresponding peak values of the Kerr retardation angle γ_{peak} were recorded (figure 8) by measuring the difference and the sum of the two split-beam intensities, $P_1 - P_2$ and $P_1 + P_2$, and substituting in equation (14). According to the quadratic equation (7), the relation between γ_{peak} and V^2_{RMS} is a straight line having a slope of $4\pi L B_k K_E^2$. Therefore, least squares curve fitting [14] has been used to determine the slope of that line (figure 8). Thus, the Kerr constant can be determined from equation (7) by

$$B_k = \frac{1}{4\pi L K_E^2} \frac{\Delta\gamma_{peak}}{\Delta V^2_{RMS}} \tag{15}$$

where $\Delta\gamma_{peak}/\Delta V^2_{RMS}$ is the slope of the fitted straight line, in rad V^{-2}.

Figure 8 dictates that the slope is 2.346×10^{-9} rad V^{-2}. Applying equation (15) to the electrode

Table 1. The field-to-voltage ratio K_E.

	$K_E(m^{-1})$			
	2 parallel plates		wire-to-plate	
H_c[a] (cm)	$R_d = 0.9$ (cm)	$R_d = 0.635$ (cm)	$R_d = 0.9$ (cm)	$R_d = 0.635$ (cm)
2	27.90	18.57	—	—
3	12.00	10.53	11.63	9.836
4	8.046	7.501	6.708	6.254
5	6.137	5.873	4.735	4.550
6	4.988	4.836	3.644	3.552
7	4.213	5.116	2.950	2.898
8	3.640	3.585	2.470	2.437

[a]For the wire-to-plate system, the radius of the wire was 0.3175 cm.

Table 2. Figure of merit for common liquids with respect to that of nitrobenzene.

Liquid	B_k[a]	ε_r[b]	Figure[c] of merit
nitrobenzene	1	35	1
water	0.0214	81	0.004
benzene	0.0027	2.29	0.64
nitrotoluene	0.5591	22.2	1.39
chloroform	−0.016	4.8	0.85

[a]As a ratio with respect to that of nitrobenzene, obtained from [5].
[b]Obtained from [15].
[c]As a ratio with respect to that of nitrobenzene.

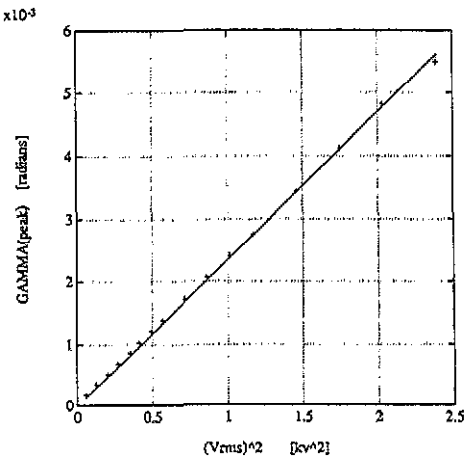

Figure 8. Kerr retardation angle of chlorotoluene versus V^2_{RMS}: +, measured values; solid line, straight-line fitting values.

configuration of cell C ($L = 0.1$ m, $d = 0.01$ m) having a field-to-voltage ratio $K_E = 100\ \mathrm{m}^{-1}$, a value of $1.867 \times 10^{-13}\ \mathrm{m\ V}^{-2}$ has been predicted for the Kerr constant of chlorotoluene. The Kerr constant of chlorotoluene is only 7.5% of that of nitrobenzene, but its dielectric constant ε_r is 6.08 [15]. Thus, its figure of merit B_k/ε_r^2 was determined to be 2.48 times that of nitrobenzene. Unlike nitrobenzene, chlorotoluene is very stable, easy to purify, less conductive, not hygroscopic and not subject to aging. For these reasons, it is selected for use in cells A and B for the proposed measuring technique.

5.3. Measured and calculated retardation angles

The two-parallel-plate and wire-to-plate gaps have been studied experimentally and analytically. For each gap, each of the two cells A and B have been placed at the centre of the distance H_c between the electrodes. Therefore, four configurations have been studied experimentally and analytically. The distance between the electrodes H_c of each configuration has been taken as variable in the range 2–8 cm.

For each of the four configurations, different values of AC voltage have been applied to the electrodes. The RMS values of the applied voltage V_{RMS} have been measured by a calibrated high-voltage potential divider, and the corresponding peak values of the Kerr retardation angle γ_{peak} have been recorded by measuring the difference and sum of the two split beams and by substituting in equation (14).

According to equation (7), the relation between γ_{peak} and V_{RMS}^2 is a straight line whose slope is $4\pi B_k L K_E^2$. Since the plot of the experimental measurements of γ_{peak} versus V_{RMS}^2 shows an almost straight line, least-squares fitting is used to determine the slope of that line, which may be called the 'experimental slope' and denoted by K_{exp}, i.e.

$$K_{exp} = \frac{\Delta\gamma_{peak}}{\Delta V_{RMS}^2} \tag{16}$$

However, the 'analytical slope', which may be denoted by K_{th}, is determined by substituting the proper values of the Kerr constant B_k, the length of the electrodes L, and the field-to-voltage ratio K_E in the following relation:

$$K_{th} = 4\pi B_k L K_E^2 \tag{17}$$

The length L of the electrodes for both systems is 0.5 m, and the Kerr constant B_k has been measured before in section 5.2 as $1.867 \times 10^{-13}\ \mathrm{m\ V}^{-2}$. However, the value of the field-to-voltage ratio K_E has been determined in table 1. Therefore, the analytical slope can be determined by equation (17).

The percentage discrepancy between the values of the experimental and the analytical slopes can be determined by

$$\text{Percentage discrepancy} = \left(1 - \frac{K_{th}}{K_{exp}}\right) \times 100\%, \tag{18}$$

The value of the percentage discrepancy, equation (18), may be considered as a measure of the accuracy of the optical measurement.

Figure 9 shows the measured peak values of the Kerr retardation angle γ_{peak} versus the measured RMS applied voltage squared V_{RMS}^2 for four different configurations. It is quite clear that the measured values are in good agreement with the straight lines for all configurations.

Figure 10 shows the measured, fitted and calculated relation between γ_{peak} and V_{RMS}^2 for a wire-to-plate system. The distance between the electrodes H_c is 7 cm and the radius of the cell R_d is 0.635 cm. In this figure, the fitted straight line is shown as a solid line which has

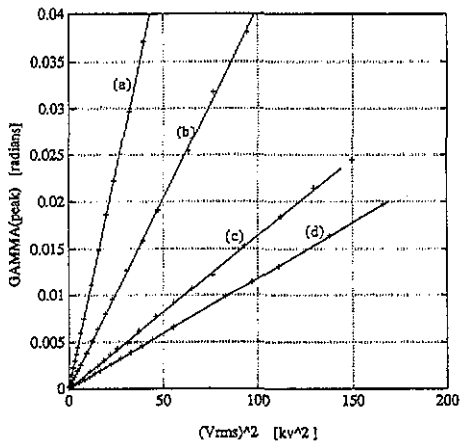

Figure 9. The measured peak values of the Kerr retardation angle γ_{peak} versus the measured RMS applied voltage squared V_{RMS}^2 for the following configurations:
(*a*) two-parallel-plate, 2 cm apart, with cell A;
(*b*) two-parallel-plate, 2 cm apart, with cell B;
(*c*) wire-to-plate, 3 cm apart, with cell A; and
(*d*) wire-to-plate, 3 cm apart, with cell B. +, measured values; solid line, second-order curve fitting.

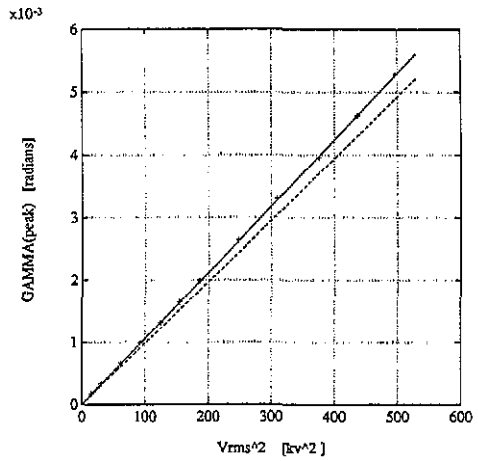

Figure 10. The measured, fitted and calculated relation between γ_{peak} and V_{RMS}^2 for wire-to-plate electrodes, 7 cm apart, with cell B: +, measured values; solid line, the fitted straight line which has a slope of $K_{exp} = 10.257 \times 10^{-12}\ \mathrm{rad\ V}^{-2}$; broken line, the theoretical line which has a calculated analytical slope of $K_{th} = 9.8501 \times 10^{-12}\ \mathrm{rad\ V}^{-2}$.

a slope $K_{exp} = 10.257 \times 10^{-12}$ radians V^{-2}. However, the broken line has an analytical slope of $K_{th} = 9.8501 \times 10^{-12}$ rad. V^{-2} determined by substituting $K_E = 2.898$ from table 1 in equation (17). Substituting in equation (18), the discrepancy between the experimental and analytical slopes was found as 7.58%. The lower the percentage discrepancy, the higher is the accuracy of the optical measurement of voltages as discussed in section 5.4.

The results of the experimental and analytical slopes and the discrepancy between them for the four configurations are summarized in tables 3–6. It is clear from tables 3–6 that the values of the experimental slope K_{exp} are higher than the corresponding values of the analytical slope K_{th} for all configurations. The maximum discrepancy between the experimental and analytical slopes is less than +8%. The positive discrepancy means that the measured retardation angle is higher than the corresponding calculated value, i.e. the actual applied field is higher than the calculated field (figure 10). This positive discrepancy may be attributed to the following:

(1) The field was assumed to be constant along the length L of the electrodes. However, at the end of the electrodes the field is intensified causing field fringing. As the length of the cells is much greater than that of the electrodes (figure 3), the fringing effect can be corrected by increasing the optical path length L subject to the uniform field in equation (7) by a factor K_L [16] greater than unity

$$K_L = \frac{\int_0^L E^2(L)\, dl}{E^2 L} \tag{19}$$

where K_L is the fringing factor. Using the dimensions of the electrodes employed in the measurements, the fringing factor has been studied by the moment method [17] and found to range from 1.03 to 1.05 according to the distance between the electrodes which varies in the range 2 to 8 cm.

(2) The fringing effect has also been ignored in determining the Kerr constant using the conventional cell. According to the electrode dimensions (10 cm long, 1 cm apart), the fringing factor K_L was found to be 1.02. Introducing this factor in equation (15) results in decreasing the Kerr constant B_k by 2%.

(3) The value of the field to voltage ratio K_E has been determined assuming that the thickness of the cell is infinitesimally small. This assumption gives an approximated value for K_E.

Therefore, the three values (B_k, L and K_E) constituting the analytical slope K_{th} of equation (17) are approximate values.

Table 3. Experimental and analytical slopes and the discrepancy between them for a two-parallel-plate arrangement with cell A.

H_c (cm)	$K_{exp} \times 10^{-12}$ (rad V^{-2})	$K_{th} \times 10^{-12}$ (rad V^{-2})	Percentage discrepancy
2	933.3	913.4	2.17
3	173.2	168.9	2.57
4	79.00	75.94	4.03
5	46.01	44.18	4.14
6	30.30	29.10	3.83
7	22.29	20.82	7.10
8	16.57	15.54	6.62

Table 4. Experimental and analytical slopes and the discrepancy between them for a wire-to-plate arrangement with cell A.

H_c (cm)	$K_{exp} \times 10^{-12}$ (rad V^{-2})	$K_{th} \times 10^{-12}$ (rad V^{-2})	Percentage discrepancy
3	163.8	158.7	3.22
4	55.27	52.93	4.69
5	28.33	26.30	7.21
6	16.55	15.58	6.22
7	10.99	10.21	7.63
8	7.650	7.155	6.91

Table 5. Experimental and analytical slopes and the discrepancy between them for a two-parallel-plate arrangement with cell B.

H_c (cm)	$K_{exp} \times 10^{-12}$ (rad V^{-2})	$K_{th} \times 10^{-12}$ (rad V^{-2})	Percentage discrepancy
2	440.7	404.5	0.62
3	133.6	130.1	2.73
4	68.68	66.15	3.83
5	42.35	40.47	4.24
6	29.23	27.44	6.53
7	20.88	19.87	5.08
8	16.17	15.07	7.27

Table 6. Experimental and analytical slopes and the discrepancy between them for a wire-to-plate arrangement with cell B.

H_c (cm)	$K_{exp} \times 10^{-12}$ (rad V^{-2})	$K_{th} \times 10^{-12}$ (rad V^{-2})	Percentage discrepancy
3	118.3	113.5	4.30
4	47.21	45.88	2.30
5	25.29	24.29	4.11
6	15.59	14.80	5.35
7	10.60	9.850	7.58
8	7.371	6.968	5.79

5.4 Optical measurement of voltage versus potential-divider measurement

For each peak value of the retardation angle, the corresponding RMS value of the voltage measured by the potential divider can be obtained by substituting the experimental slope K_{exp} in the following relation

$$V_{div} = \frac{\sqrt{\gamma_{peak}}}{\sqrt{K_{exp}}} \tag{20}$$

where V_{div} is the actual RMS voltage measured by the

potential divider. However, the corresponding optically measured voltage is determined by

$$V_{opt} = \frac{\sqrt{\gamma_{peak}}}{\sqrt{K_{th}}}. \quad (21)$$

The percentage error between the voltage measured by the potential divider and by the proposed optical technique may be defined by

$$\text{voltage error} = \frac{V_{div} - V_{opt}}{V_{div}} \times 100\%. \quad (22)$$

Substituting for V_{div} and V_{opt} yields

$$\text{voltage error} = (1 - \sqrt{K_{exp}/K_{th}}) \times 100\%. \quad (23)$$

Since the maximum discrepancy between K_{exp} and K_{th} is less than 8% as shown in tables 3–6, the voltage error is less than 3.9%.

6. Conclusions

On the basis of the present analysis, the following conclusions may be drawn about the proposed new laser voltmeter:

(1) A new technique has been proposed for remote measurement of high conductor voltages. It is based on a new Kerr cell having no electrodes. This technique can be used for measuring a wide range of voltages by choosing a suitable location for the cell underneath the conductor.
(2) Because the cell is surrounded by air, a figure of merit for the optically active liquid filling the cell has been proposed. The figure of merit is a function of both the dielectric and Kerr constants of the liquid.
(3) A promising liquid (chlorotoluene), having no previous Kerr effect applications, has been employed in the new cell because its figure of merit is much higher than that of nitrobenzene which has the highest Kerr constant among the common known liquids.
(4) Since the Kerr constant of chlorotoluene is not reported in the literature, it has been measured using a conventional Kerr cell.
(5) A new optical system has been used for measuring the Kerr retardation angle. With this system a Kerr retardation angle of 10 mill-degrees was measured even though the laser source has a sensible intensity of noise ripple of 16.7%.
(6) The voltage applied to two-parallel-plate and wire-to-plate gaps has been measured optically and by a calibrated potential divider. The maximum error for the voltage measurements was 3.9%. The error may be attributed to the fringing effect at the end of the electrodes. Therefore, a correction factor for the finite length of the electrodes has been proposed.
(7) The proposed measuring technique calls for a determination of the ratio between the field inside the cell and the voltage to be measured. This ratio depends on the position of the cell relative to the high-voltage electrode. Therefore this technique can be used in high-voltage transmission lines, substations or laboratories by placing the cell in an appropriate location near the high-voltage electrode.

7. Acknowledgments

One of us (MA-E) wishes to acknowledge the support he received from Michigan Technical University (MTU) to achieve the experimental phase of this work at the high-voltage laboratory of MTU. The second author wishes to acknowledge King Fahd University of Petroleum and Minerals for the support he received during the progress of this work.

The authors wish to acknowledge the reviewers for their instructive comments that enhanced the clarity of the paper.

References

[1] Saleh B A and Teich M C 1991 *Fundamentals of Photonics* (New York: Wiley)
[2] Zahn M, Takada T and Voldman S 1983 Kerr electro-optic field mapping measurements in water using parallel cylindrical electrodes *J. Appl. Phys.* **54** 4749–61
[3] Wunsch D C 1964 Kerr cell measuring system for high voltage pulses *Rev. Sci. Instrum.* **35** 816–20
[4] Hebner R E, Malewski R A and Cassidy E C 1977 Optical methods of electrical measurements at high voltage levels *Proc. IEEE* **65** 1524–48
[5] Hecht E and Zajac A 1974 *Optics* (Reading, MA: Addison-Wesley)
[6] Bright A W, Makin B and Pearmain A J 1969 Field distribution in nitrobenzene using the Kerr effect *J. Phys. D: Appl. Phys.* **2** 447–51
[7] Cassidy E C, Hebner R E, Zahn M and Sojka R J 1974 Kerr effect studies of an insulating liquid under varied high voltage conditions *IEEE Trans. Elec. Insul.* **9** 43–56
[8] Faeger N A F and Young L 1989 High voltage sensor employing an integrated optics Mach–Zehnder interferometer in conjunction with capacitive divider *J. Lightwave Technol.* **7** 229–34
[9] Zhu Z H, Weber J-P, Wang S Y and Wang S 1986 New measurement technique: CW electro-optic probing of electric fields *Appl. Phys. Lett.* **49** 432–4
[10] Massey G A, Erickson D C and Kadlec R A 1974 Electromagnetic field components: their measurement using linear electrooptic and magnetooptic effects *Appl. Opt.* **14** 2712–9
[11] Abdel-Salam M 1990 *Electric Fields in High Voltage Engineering: Theory and Practice* ed Khalifa (New York: Dekker)
[12] Singer H, Steinbigler H and Weiss P 1974 A charge simulation method for the calculation of high voltage fields *IEEE Trans. PAS* **9** 1660–8
[13] Abdel-Salam M, Wiitanen D O and Abd-Elsalam M 1989 Electric fields in a Kerr-cell placed underneath a coronating transmission-line conductor *Proc. 6th*

Int. Symp. on High Voltage Engineering (ISH-89) (New Orleans) Paper 50.09
[14] James M, Smith G and Woldford J 1985 *Applied Numerical Methods for Digital Computation* 3rd edn (New York: Harper and Row)
[15] Weast R C 1989–90 *Handbook of Chemistry and Physics* 70th edn (Boca Raton, FL: Chemical Rubber Company)
[16] Thacher P 1976 Optical effects of fringing fields in Kerr cells *IEEE Trans. Elec. Insul.* **11** 40–50
[17] Harrington R F 1968 *Field Computation by Moment Methods* (New York: Macmillan)